

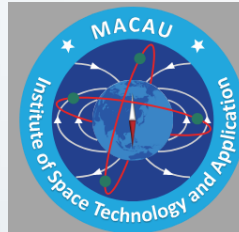
Reconstruction of 3-D Core Flow from Geomagnetic Satellite Data

Yufeng Lin , Jinfeng Li (SUSTech)

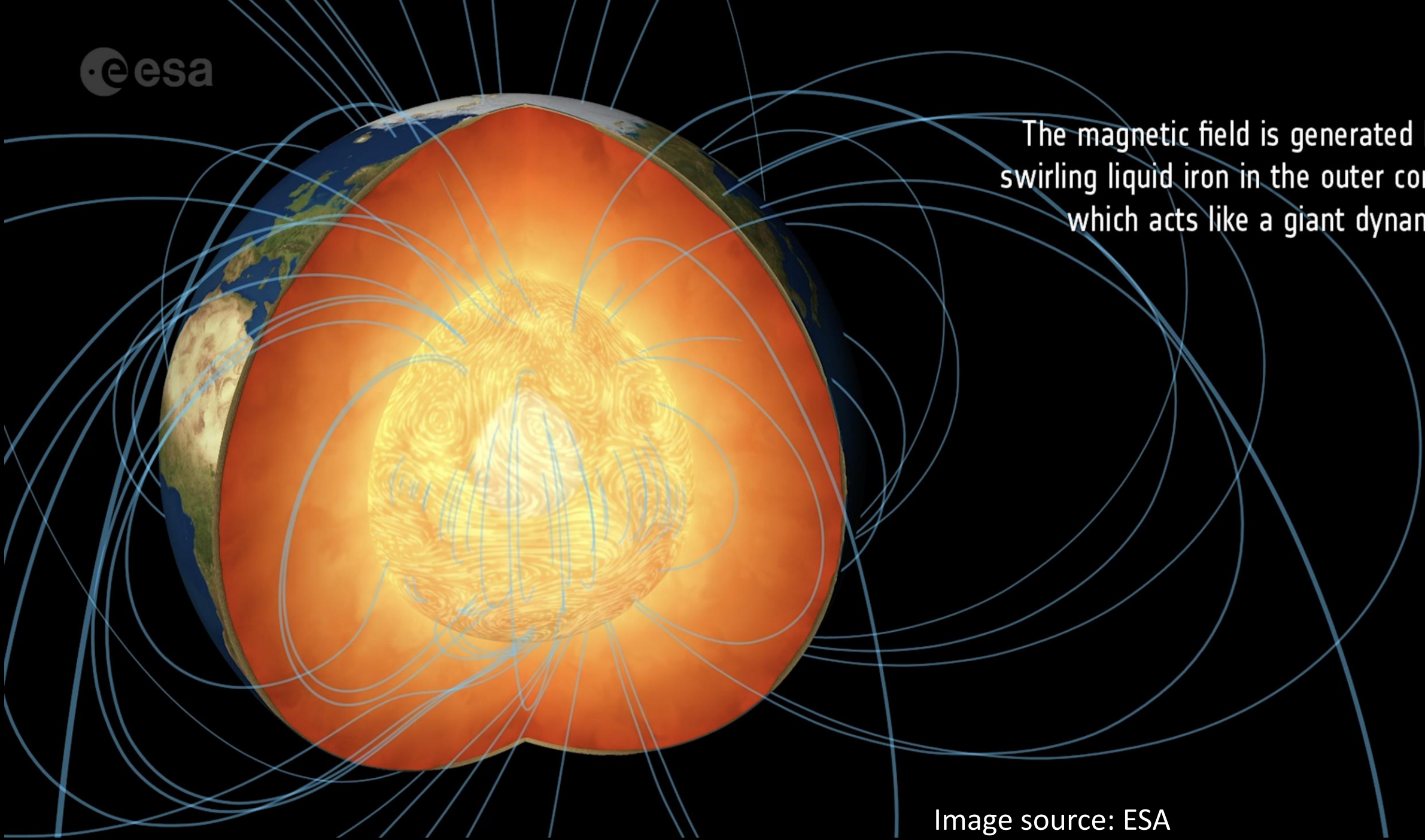
Keke Zhang (MISTA)



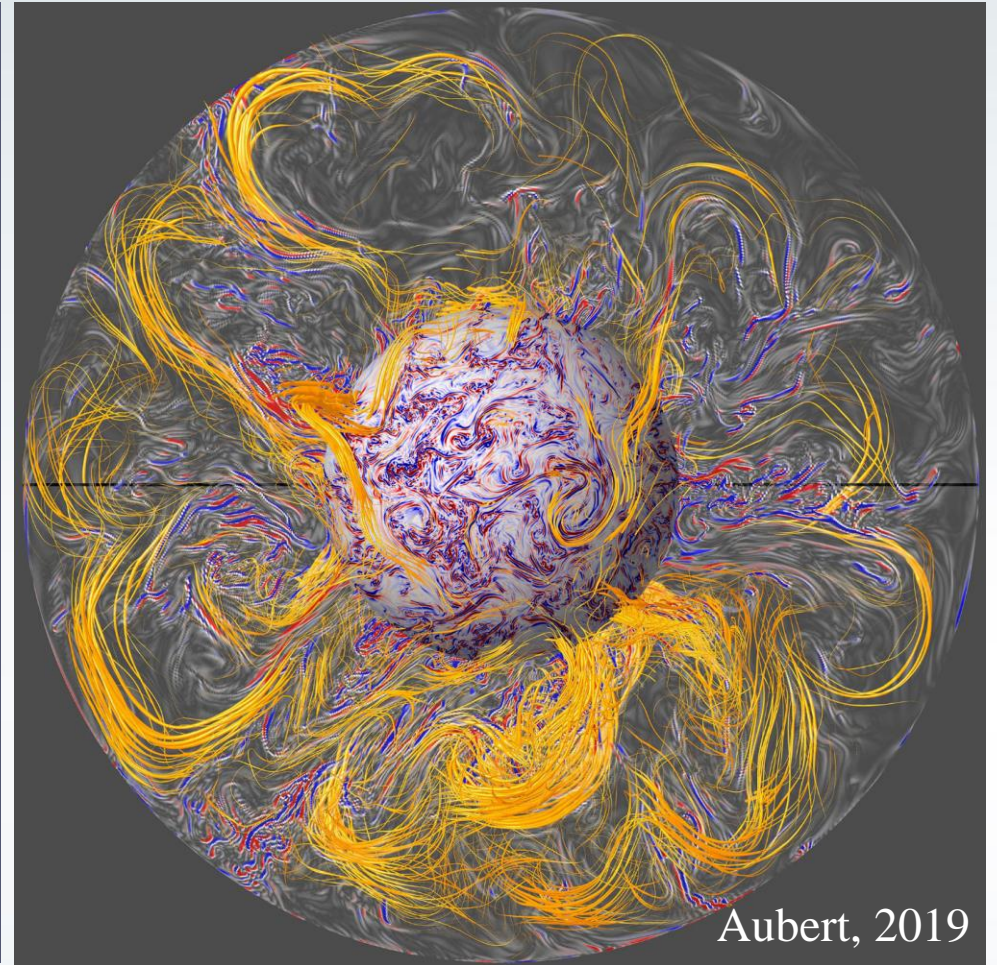
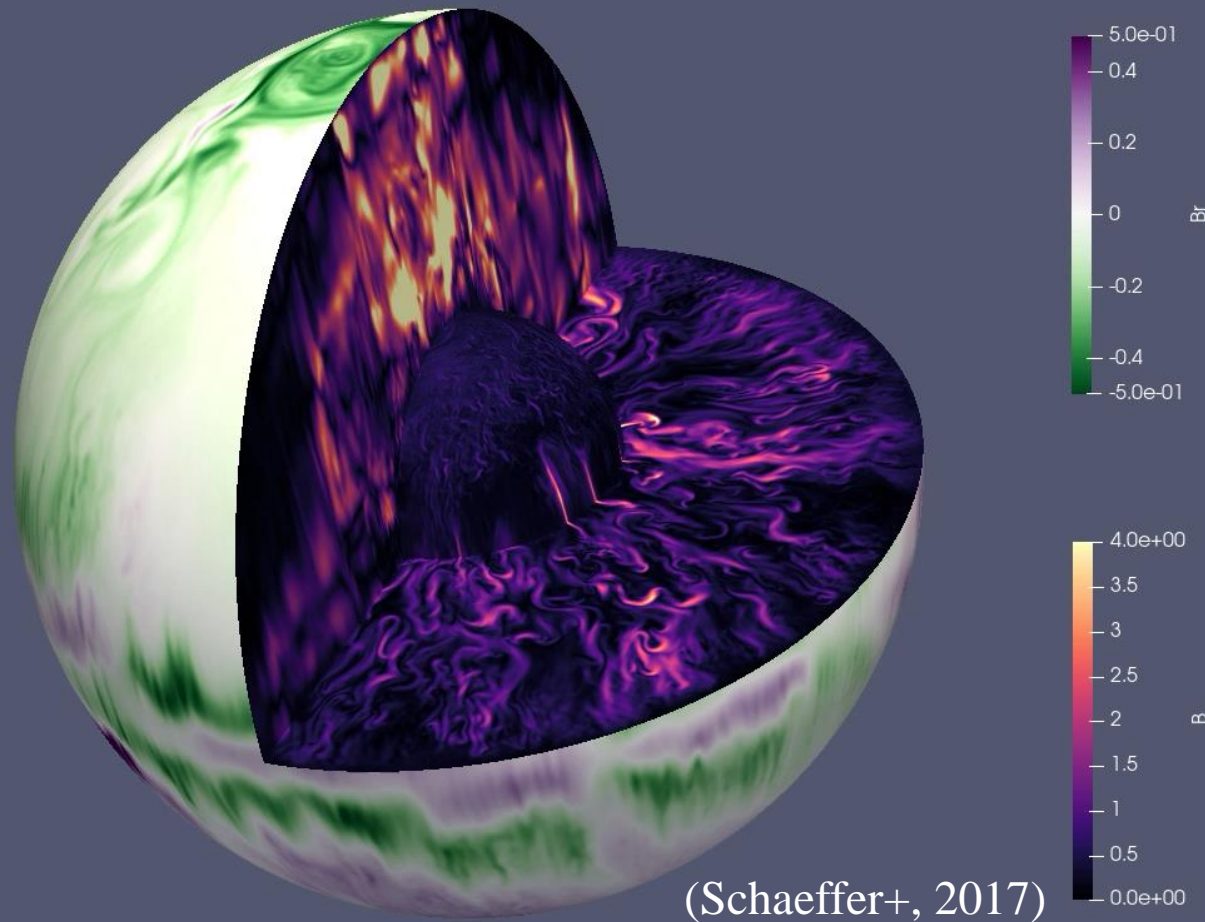
南方科技大学
SOUTHERN UNIVERSITY OF SCIENCE AND TECHNOLOGY



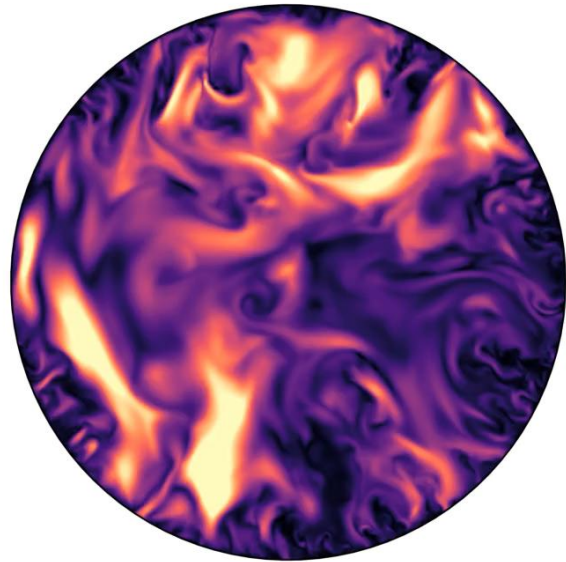
澳門空間技術與應用研究院
Macau Institute of Space Technology and Application



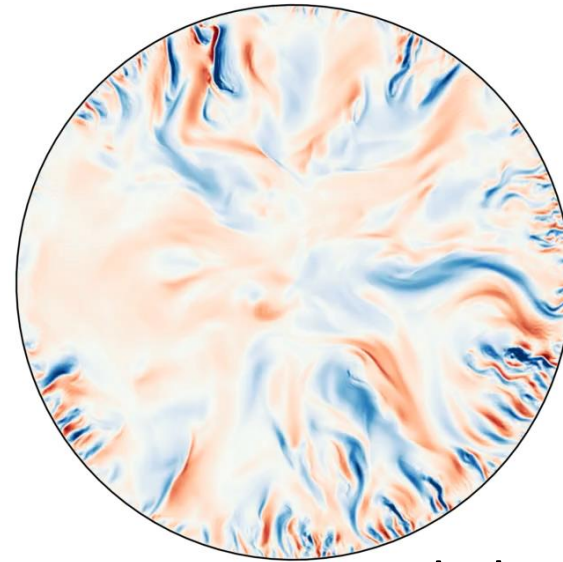
The magnetic field is generated by swirling liquid iron in the outer core, which acts like a giant dynamo



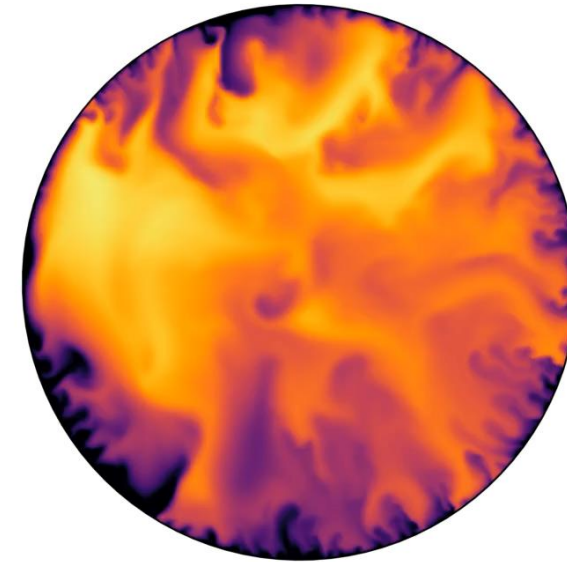
Numerical simulations have significantly advanced our understanding of the geodynamo and core dynamics.



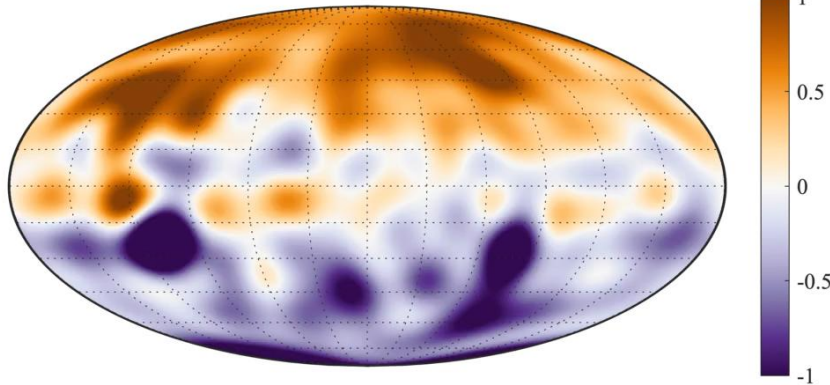
Magnetic field



Radial velocity



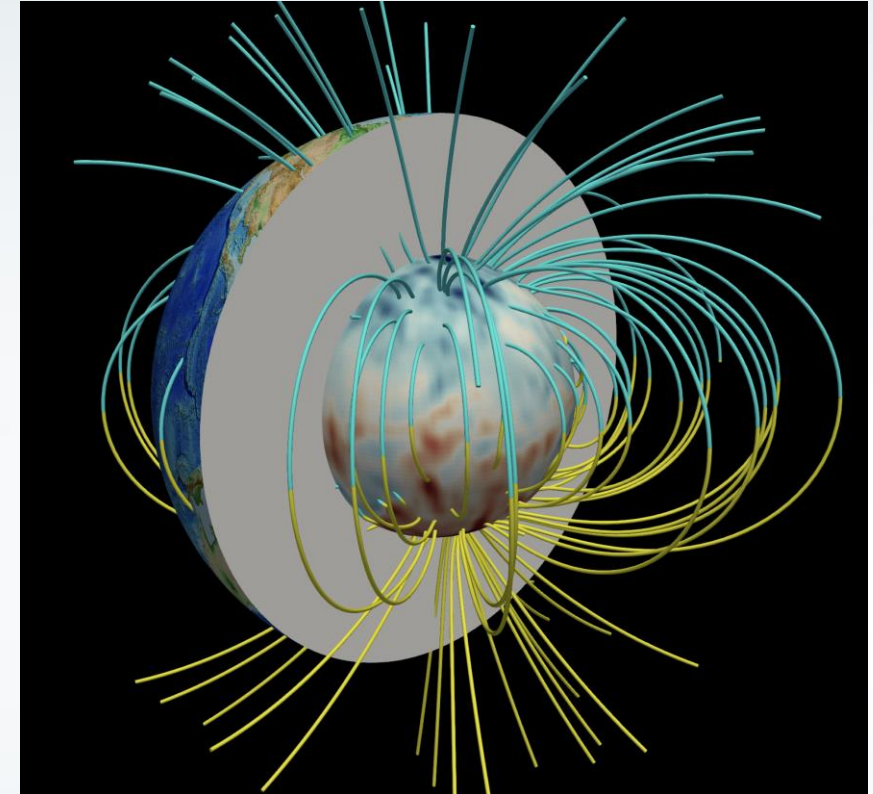
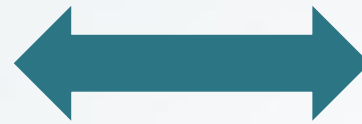
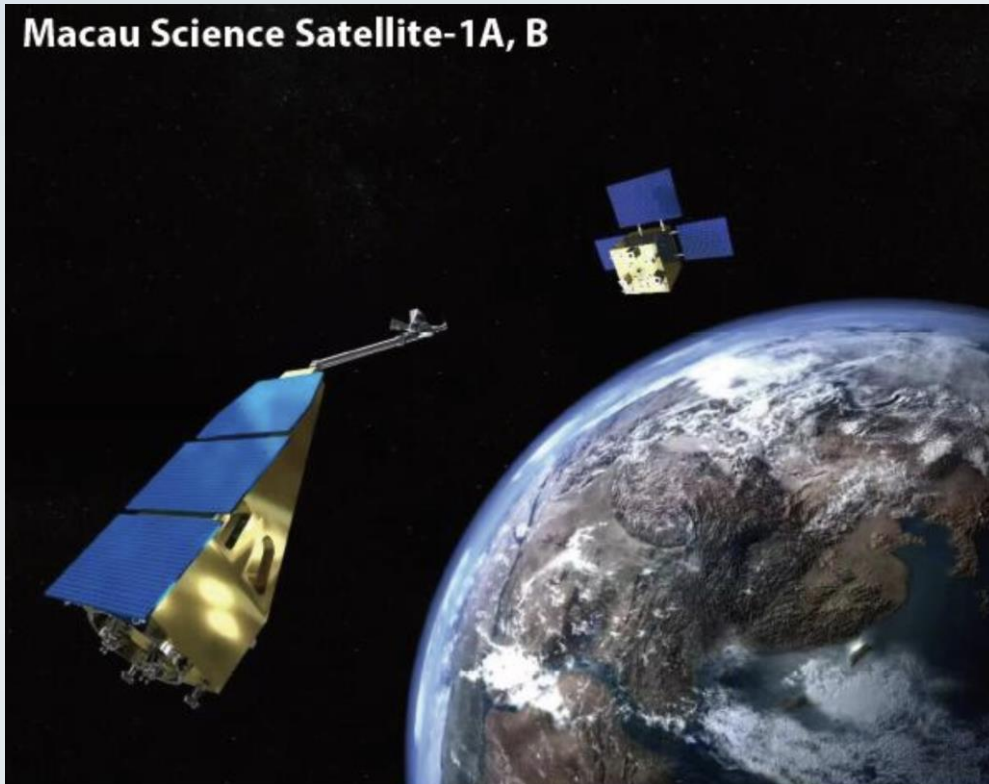
Temperature



**Dynamo simulations at
Ekman number $E=10^{-8}$
(Realistic value $E \sim 10^{-15}$)**

It remains a challenge to reach the realistic parameter regime.

Continuous satellite measurements of the Earth's magnetic field have been available since 1999.



**How to constrain the core dynamics using
geomagnetic observations?**

❖ Kinematic inversion

(Robert & Scott, 1965; Jackson, 1997; Holme, 2015; Kloss & Finlay, 2019; Whaler et al., 2022, Li, Lin & Zhang, 2023)

$$\frac{\partial \mathbf{B}}{\partial t} = \nabla \times (\mathbf{u} \times \mathbf{B}) + \eta \nabla^2 \mathbf{B} \xrightarrow{\text{Frozen flux approximation}} \boxed{\frac{\partial B_r}{\partial t} = -\nabla_{\mathbf{h}} \cdot (\mathbf{u}_{\mathbf{h}} B_r)}$$

Can only infer large-scale 2-D core surface flow.

❖ Geomagnetic data assimilation

(Kuang+, 2009; Fournier+, 2013; Li & Jackson 2014; Sanchez et al., 2019; Li, Lin & Zhang, 2023)

Can recover 3-D core dynamics and make predictions the evolution of core field, but it requires realistic geodynamo models.

3-D Core-flow inversion

$$\frac{\partial \mathbf{u}}{\partial t} + \cancel{\mathbf{u} \cdot \nabla \mathbf{u}} + 2\boldsymbol{\Omega} \times \mathbf{u} = -\frac{1}{\rho} \nabla p + \cancel{\frac{ag_0 r}{r_0} \Theta} + \cancel{v \nabla^2 \mathbf{u}} + \frac{1}{\rho \mu} (\nabla \times \mathbf{B}) \times \mathbf{B}$$

Rotation-dominated flow

$$\frac{\partial \mathbf{u}}{\partial t} + 2\boldsymbol{\Omega} \times \mathbf{u} + \frac{1}{\rho} \nabla p = 0, \quad \nabla \cdot \mathbf{u} = 0$$

Inertial modes

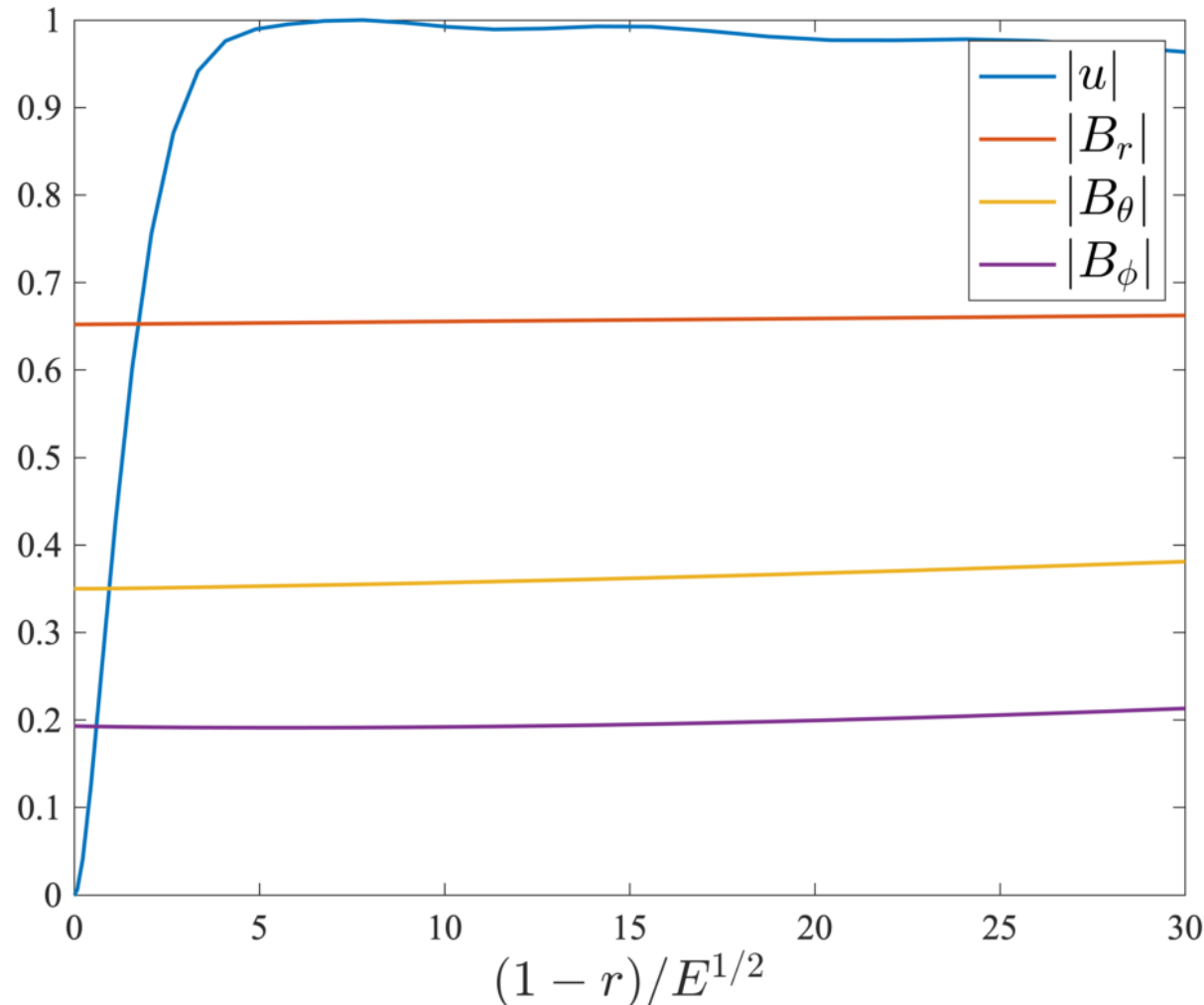
Analytical solutions
(Zhang & Liao, 2017)

$$\mathbf{u}(r, \theta, \phi, t) = \sum_{mnk} C_{mnk}(t) \mathbf{u}_{mnk}(r, \theta, \phi)$$

Observations

$$\frac{\partial \mathbf{B}}{\partial t} = \nabla \times (\mathbf{u} \times \mathbf{B})$$

(Kloss & Finlay, 2019)



All 3 components of magnetic field show negligible changes across the velocity boundary layer.

Therefore, we made use of three-components magnetic induction equation.

$$\frac{\partial \mathbf{B}}{\partial t} = \nabla \times (\mathbf{u} \times \mathbf{B})$$

$$\frac{\partial \mathbf{B}}{\partial t} = \nabla \times (\mathbf{u} \times \mathbf{B})$$

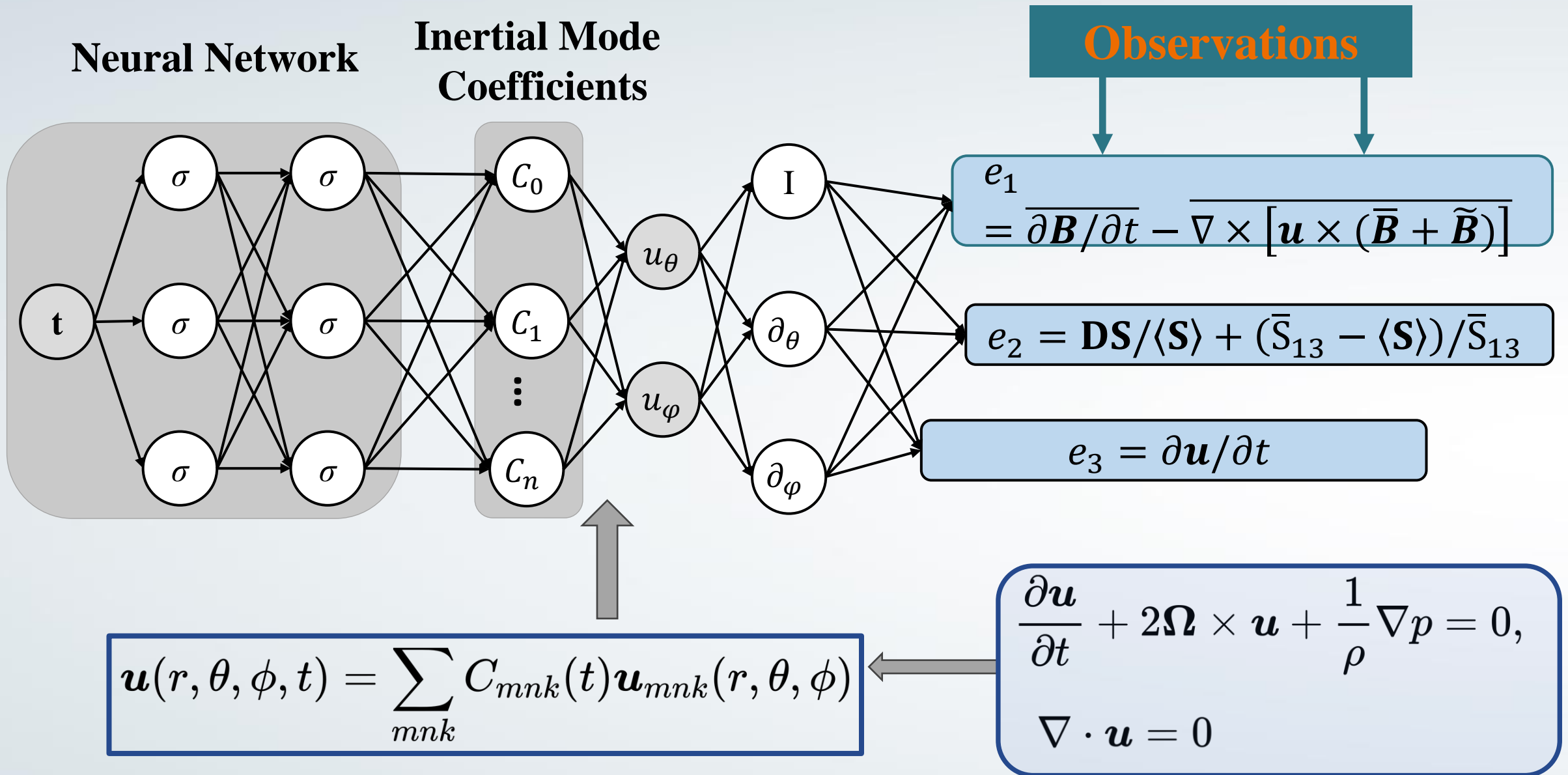
$$\mathbf{u}(\mathbf{r}, t) = \sum_{k=1}^K c_k^G(t) G_{2k-1}(\mathbf{r}) \hat{\Phi} + \sum_{k=1}^K \sum_{m=1}^M \sum_n c_{mnk}^S(t) \Re[u_{mnk}^S(\mathbf{r})] + \sum_{k=0}^K \sum_{m=1}^M \sum_n c_{mnk}^A(t) \Re[u_{mnk}^A(\mathbf{r})]$$

Axisymmetric
geostrophic mode

Equatorially
symmetric modes

Equatorially
antisymmetric modes

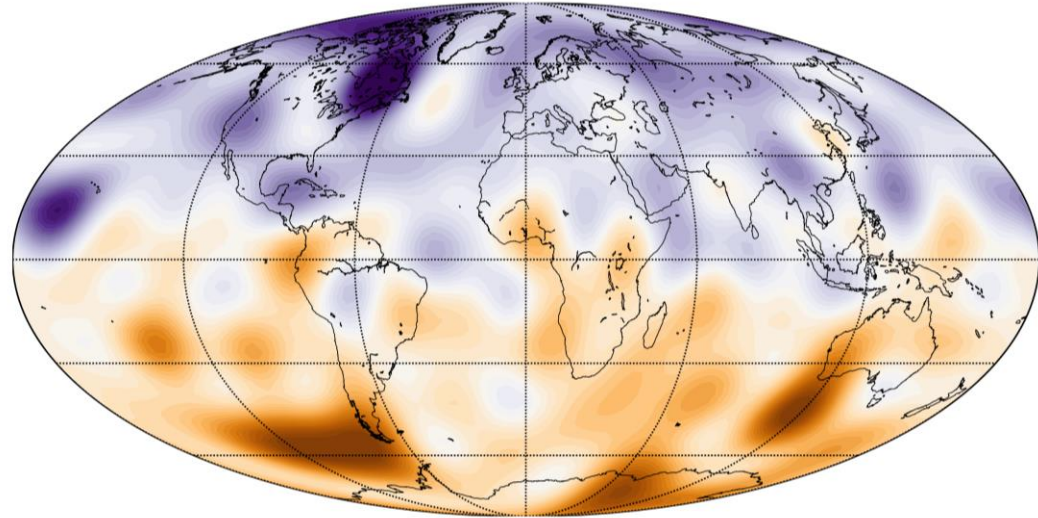
- **Inertial modes are truncated at $K = M = 10$.**
- **Only the slowest E^S and E^A modes are included, i.e. $n = 1$.**
- **We use 220 inertial modes in total.** [Kloss & Finlay (2019) used 4720 inertial modes with $K = 10, M = 20, N = 60$.]



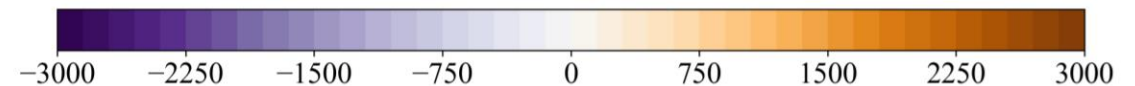
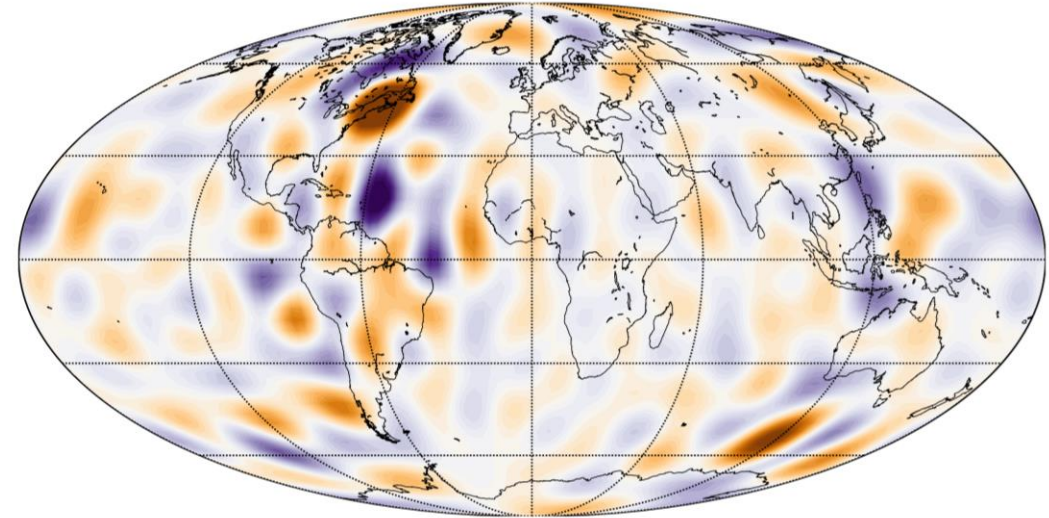
Dynamo simulation

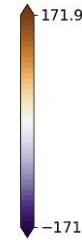
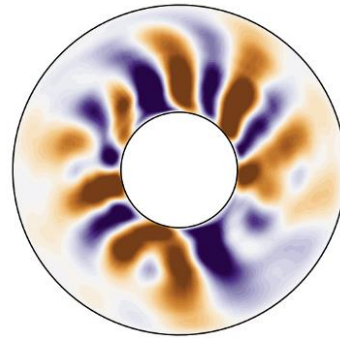
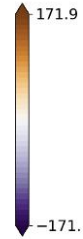
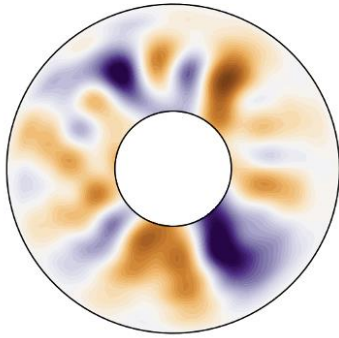
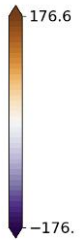
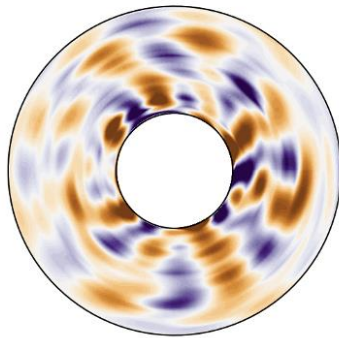
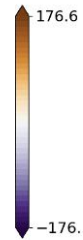
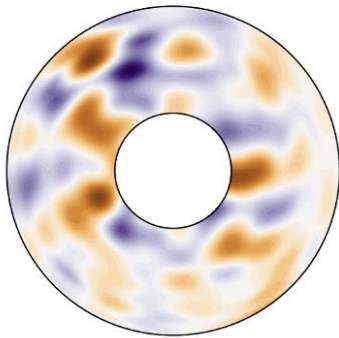
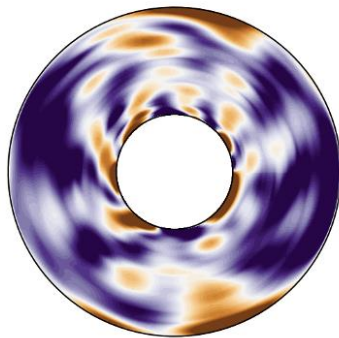
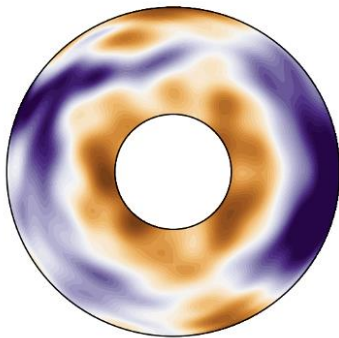
Control Parameters				Time-averaged Output parameters		
E	Pr	Pm	Ra	Λ	Rm	χ^2
10^{-5}	1.0	3.0	2.2×10^8	36	803	1.2

Br at CMB



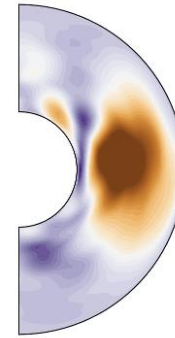
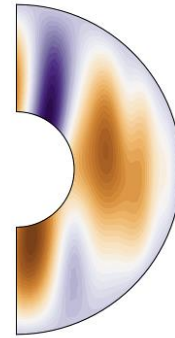
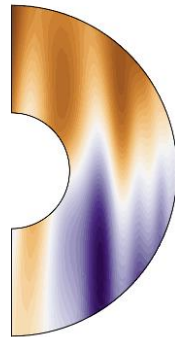
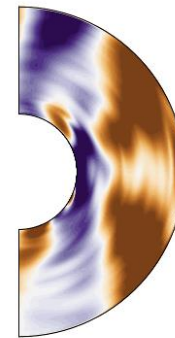
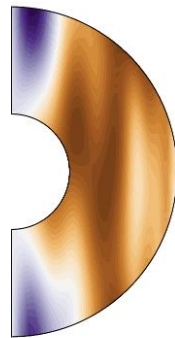
$\partial Br / \partial t$ at CMB



u_r  u_θ  u_ϕ 

Inverted

Reference

 u_r  u_θ  u_ϕ 

Inverted

Reference

Correlation coefficients

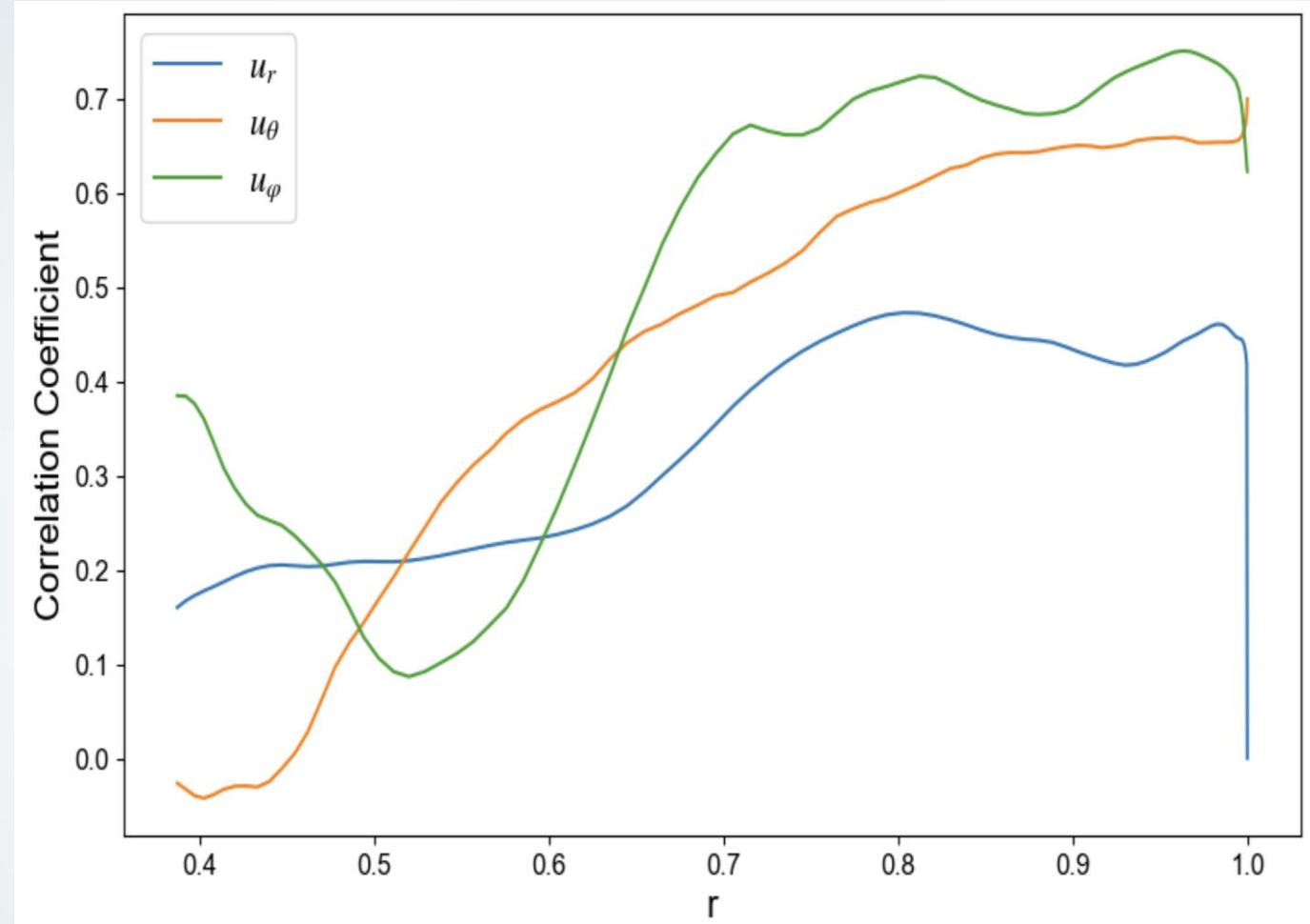
$$C_r(r) = \frac{\sum_{N_s} u_r(r, \theta, \varphi) u_r^{\text{ref}}(r, \theta, \varphi)}{\sqrt{(\sum_{N_s} u_r(r, \theta, \varphi) u_r(r, \theta, \varphi)) (\sum_{N_s} u_r^{\text{ref}}(r, \theta, \varphi) u_r^{\text{ref}}(r, \theta, \varphi))}},$$

$$C_\theta(r) = \frac{\sum_{N_s} u_\theta(r, \theta, \varphi) u_\theta^{\text{ref}}(r, \theta, \varphi)}{\sqrt{(\sum_{N_s} u_\theta(r, \theta, \varphi) u_\theta(r, \theta, \varphi)) (\sum_{N_s} u_\theta^{\text{ref}}(r, \theta, \varphi) u_\theta^{\text{ref}}(r, \theta, \varphi))}},$$

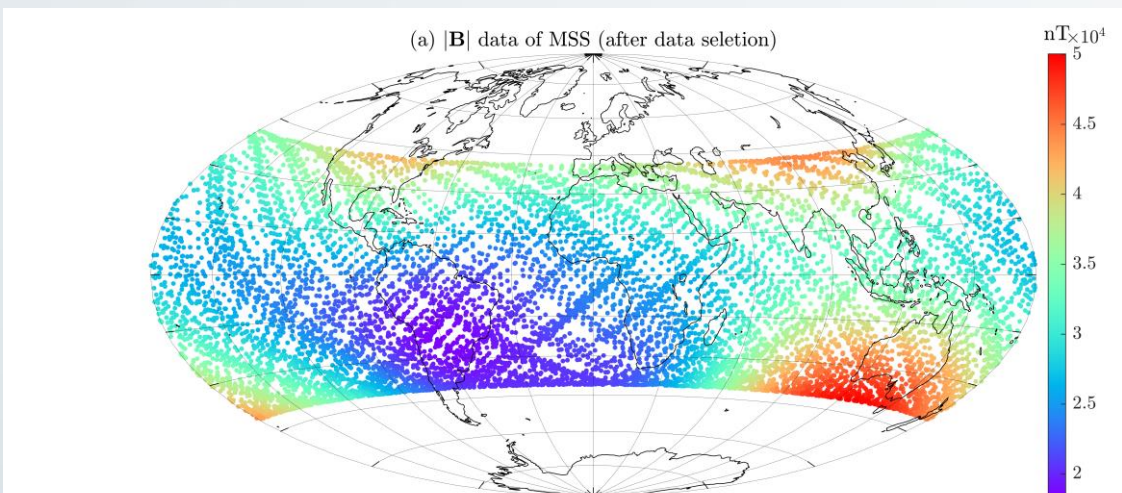
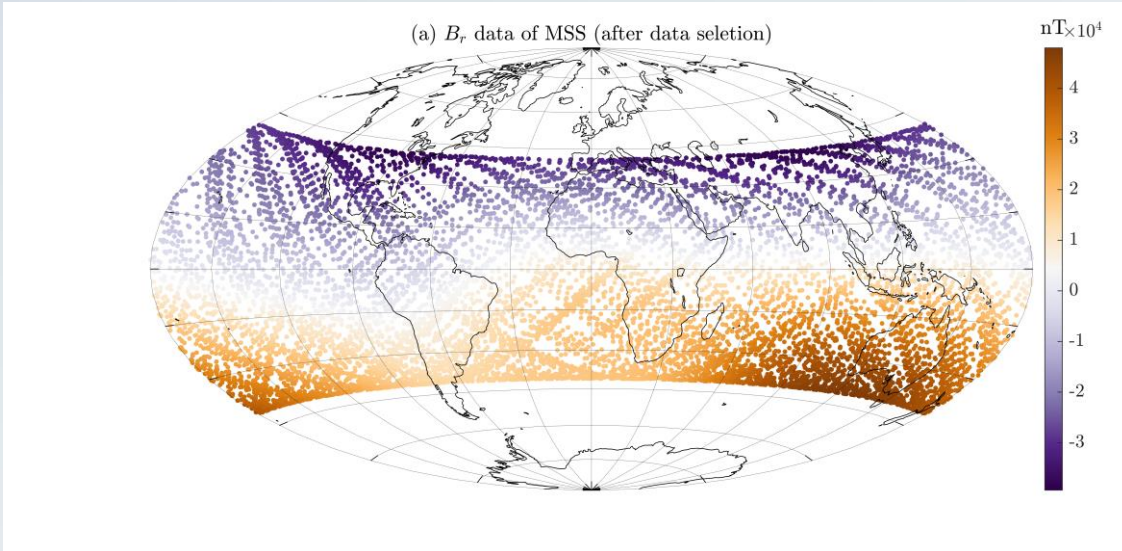
$$C_\varphi(r) = \frac{\sum_{N_s} u_\varphi(r, \theta, \varphi) u_\varphi^{\text{ref}}(r, \theta, \varphi)}{\sqrt{(\sum_{N_s} u_\varphi(r, \theta, \varphi) u_\varphi(r, \theta, \varphi)) (\sum_{N_s} u_\varphi^{\text{ref}}(r, \theta, \varphi) u_\varphi^{\text{ref}}(r, \theta, \varphi))}} \quad \square$$

ICB

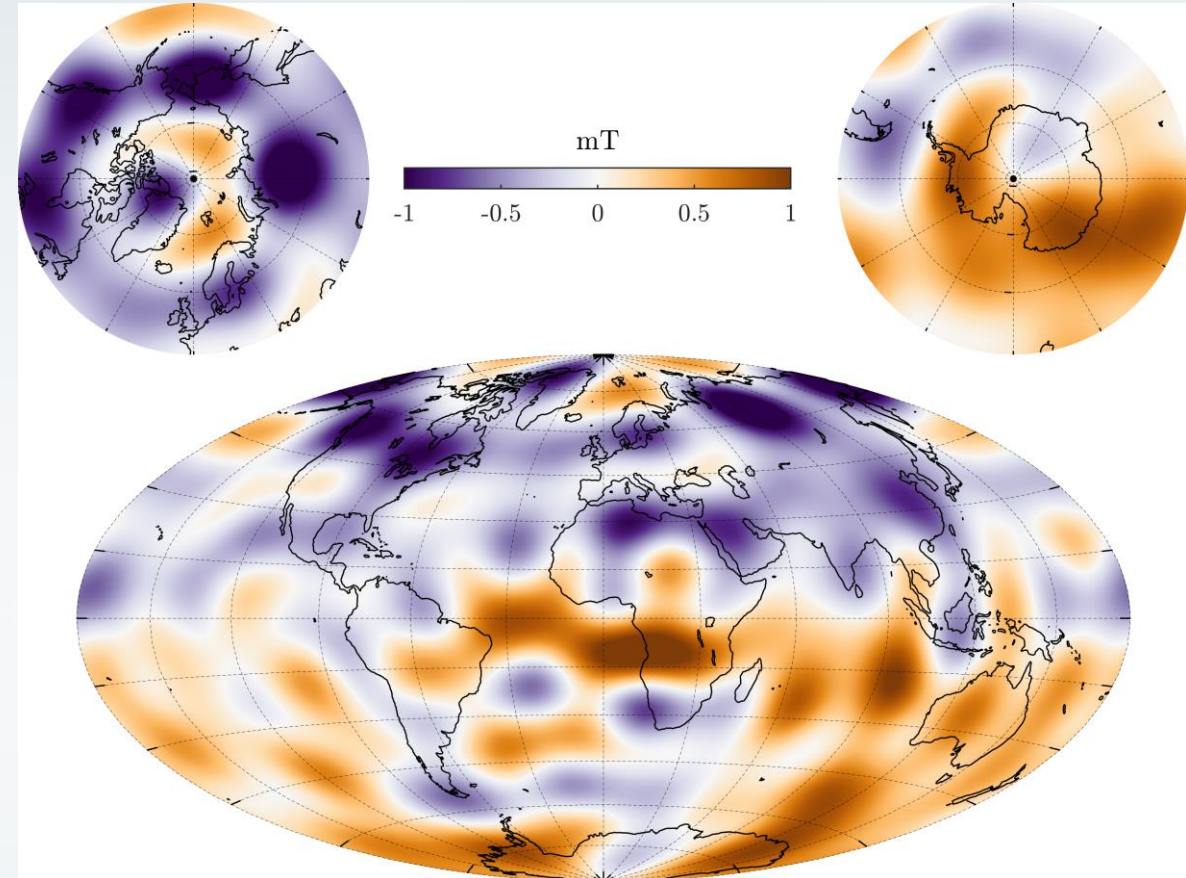
CMB



MSS-1 vector magnetic field data (2023/08/18-09/30)



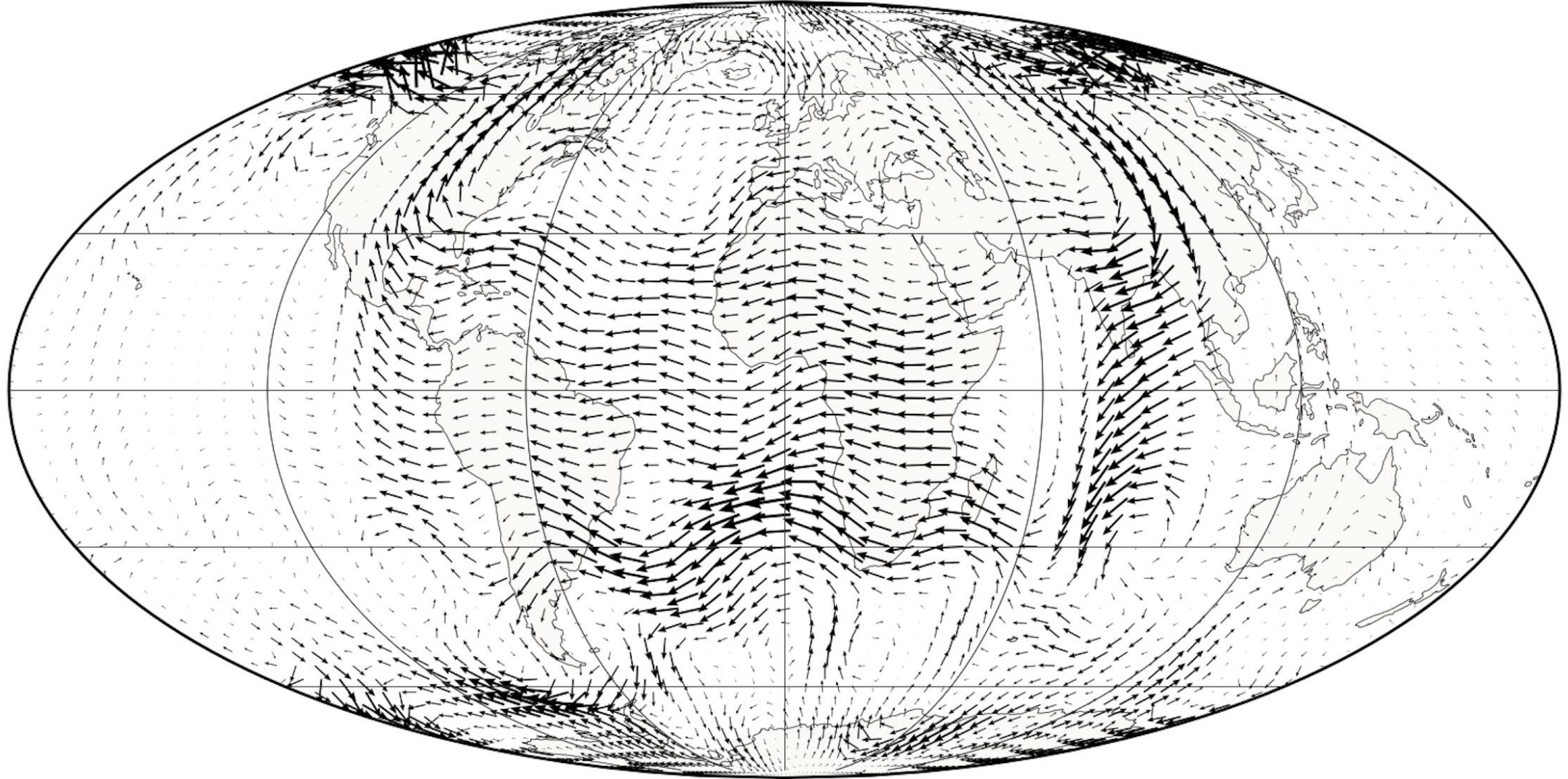
Core field B_r at CMB (MSS1+Swarm A)



+

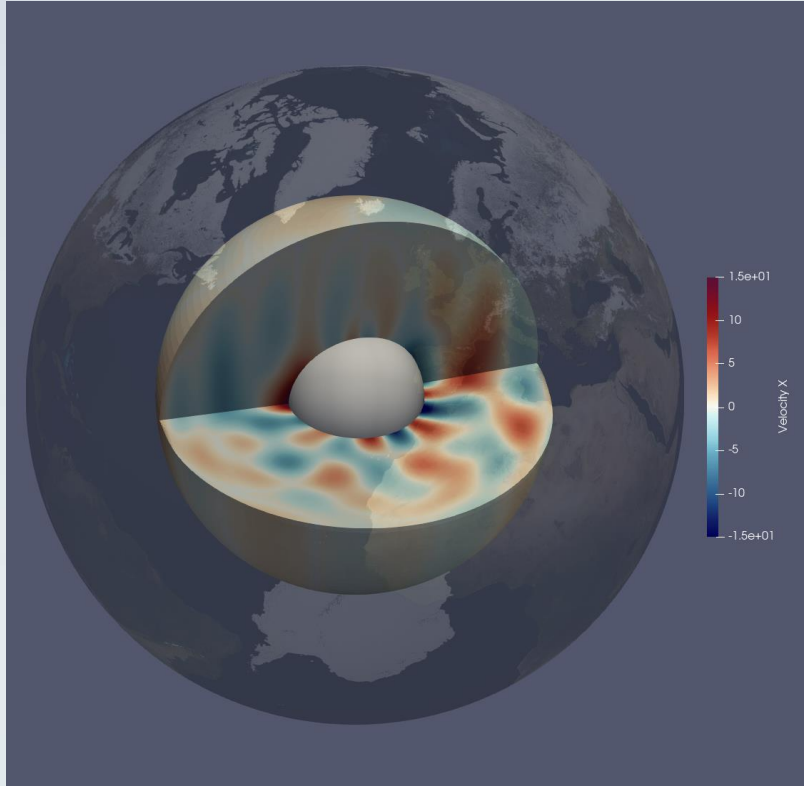
CHAOS-7 MF and SV

2023.0

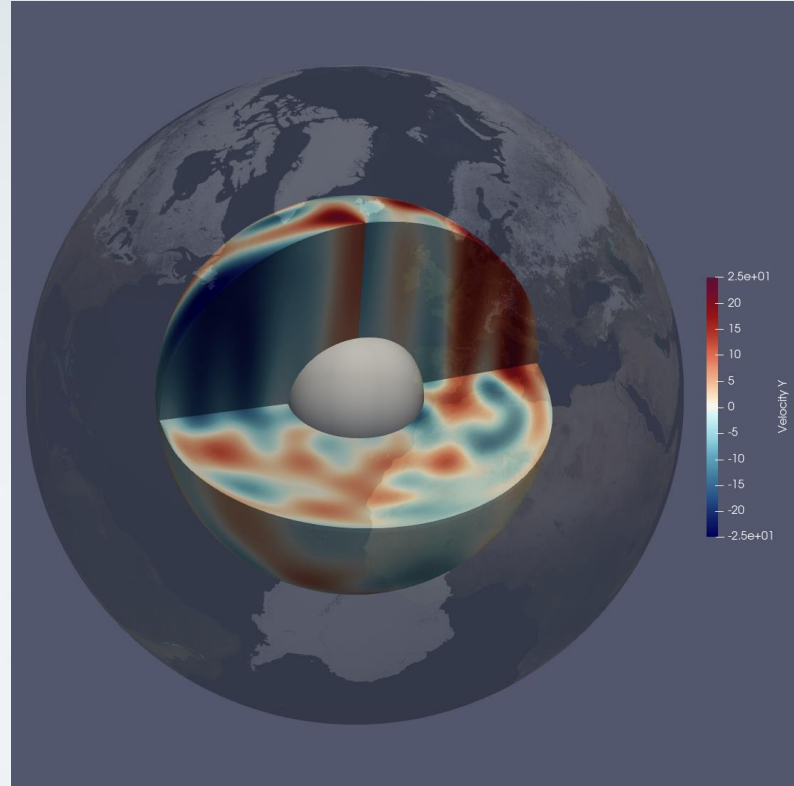


→
25 km/yr

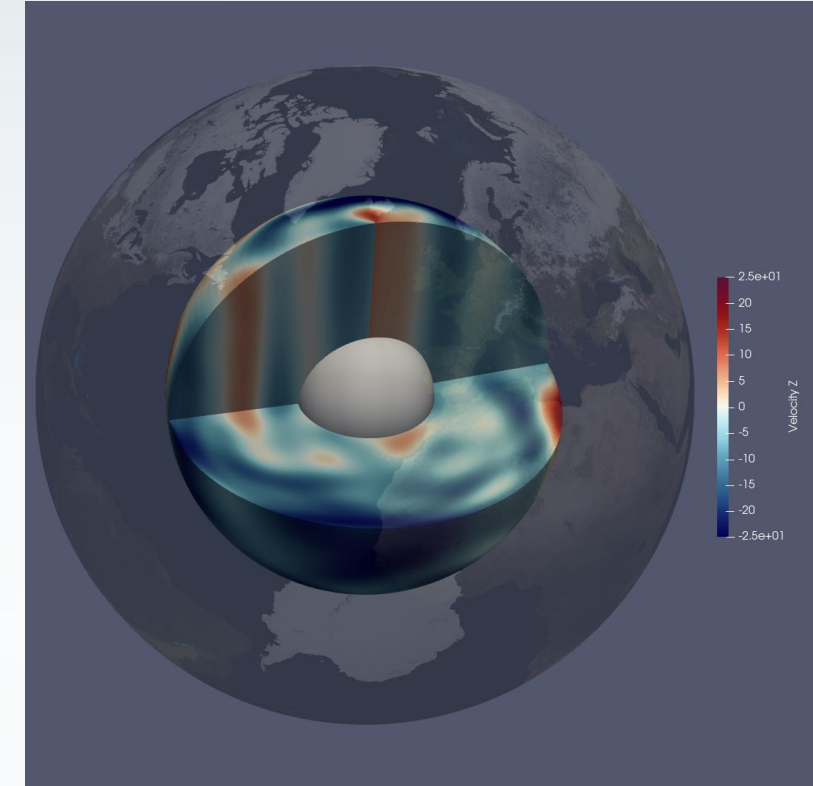
3-D flow visualizations



u_r

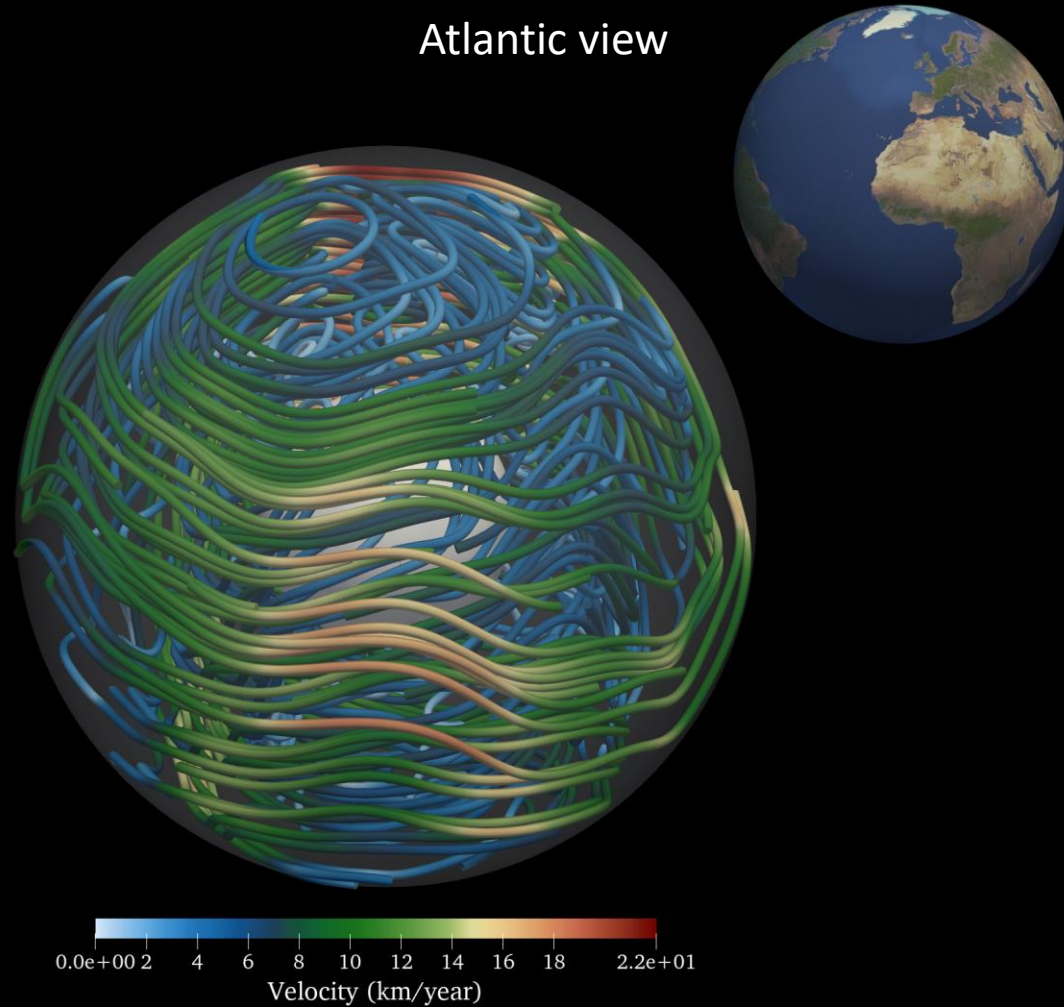


u_θ

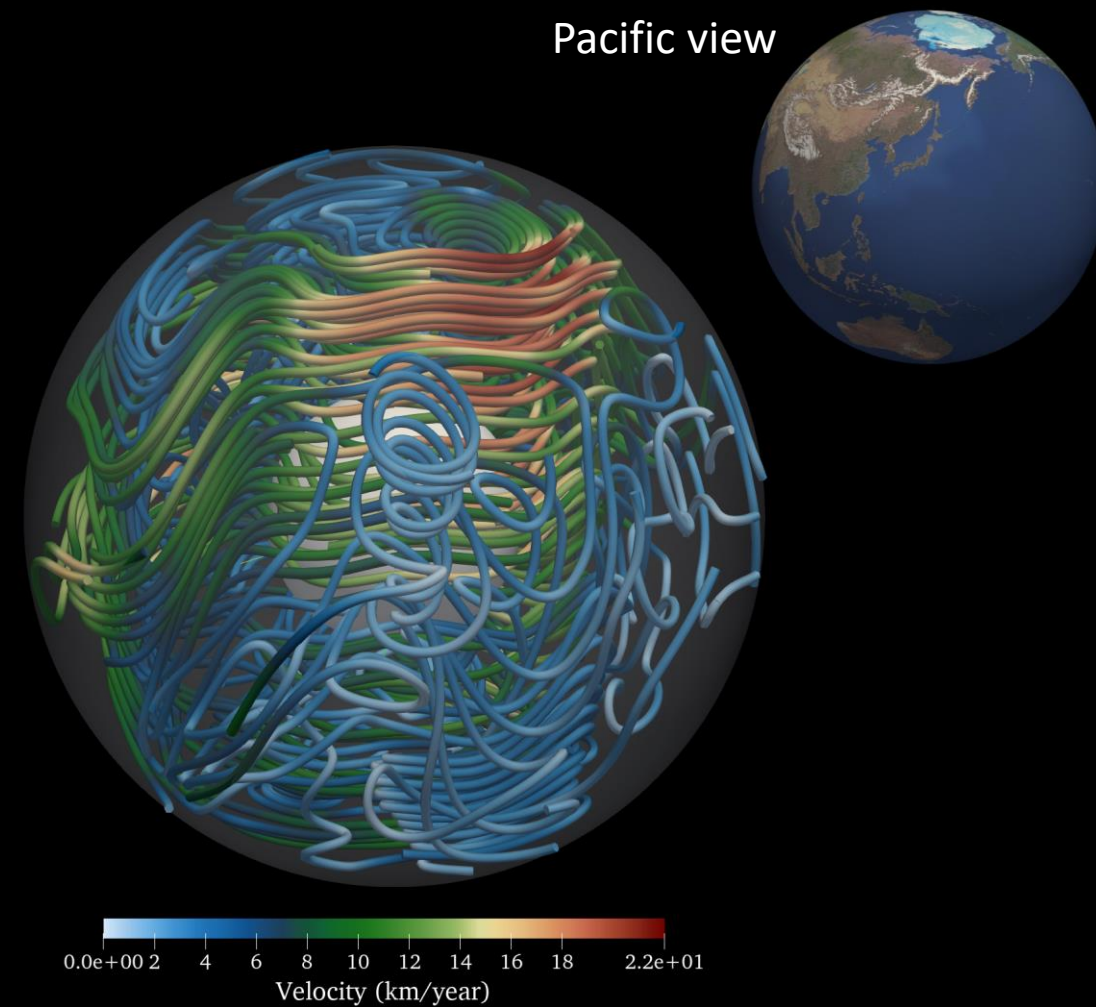


u_ϕ

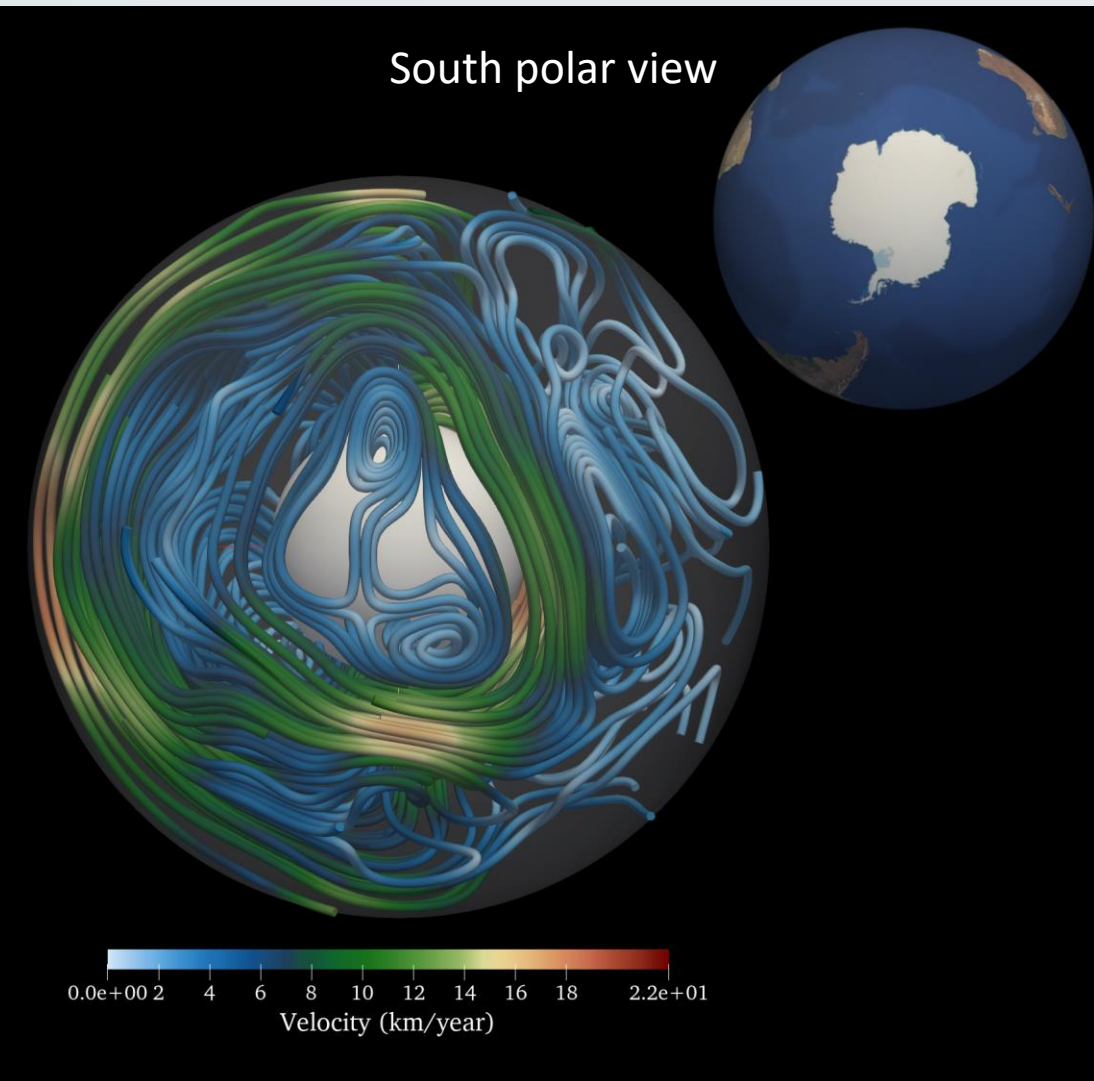
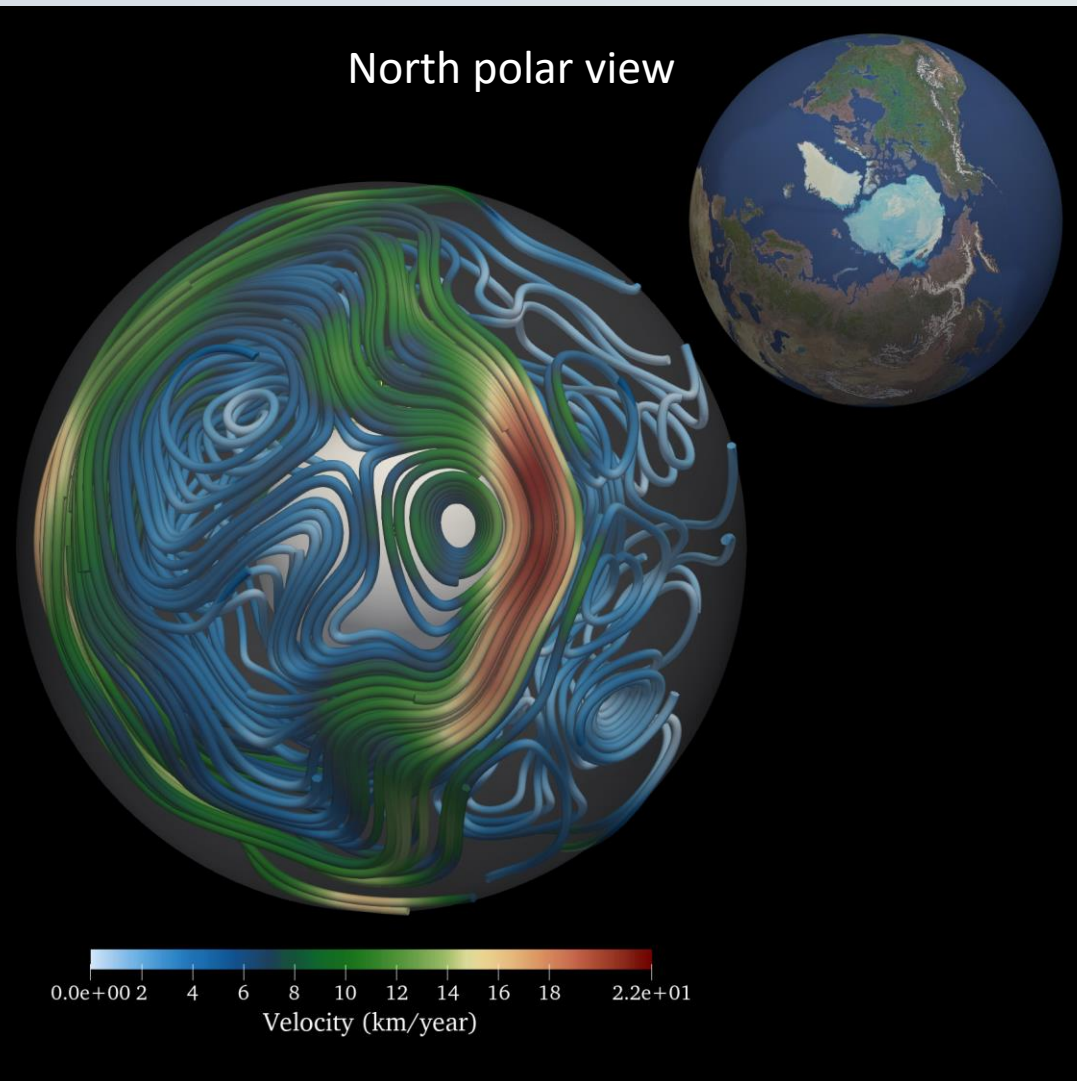
Atlantic view



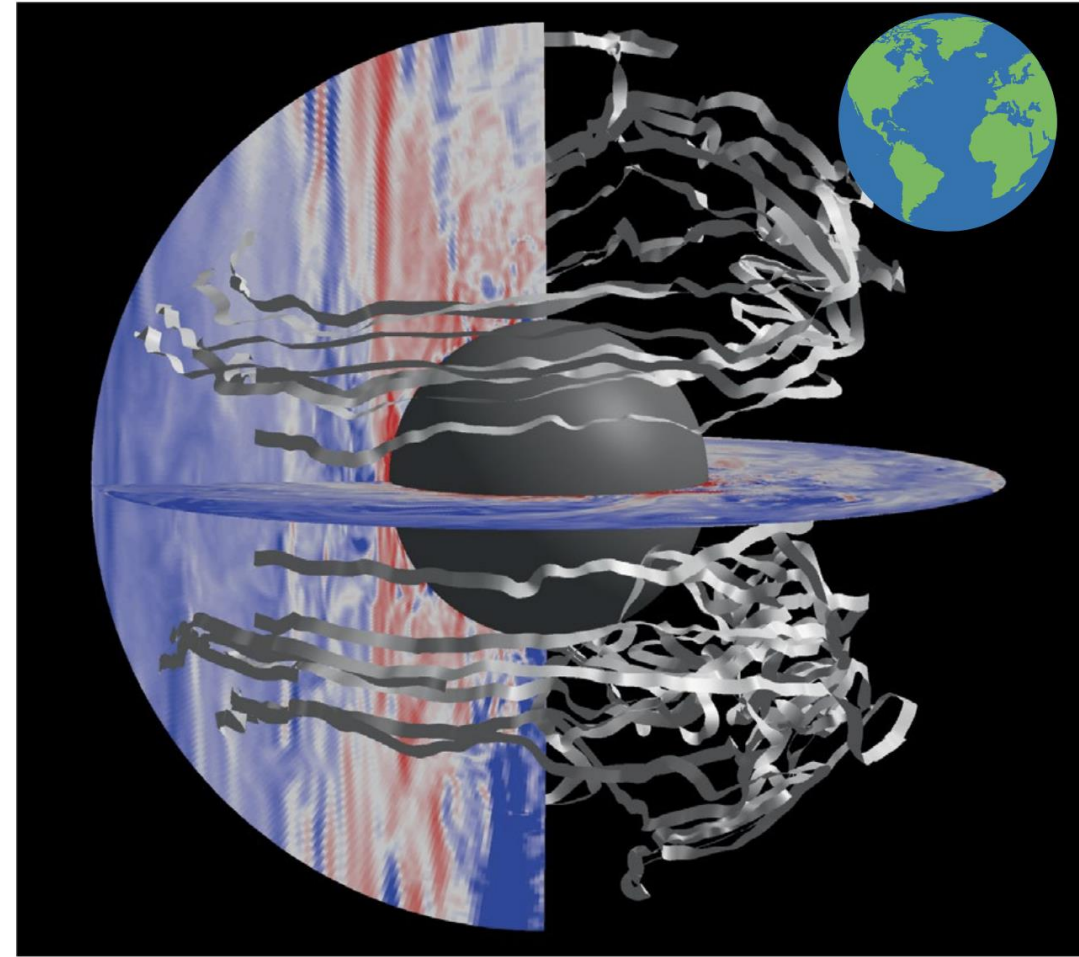
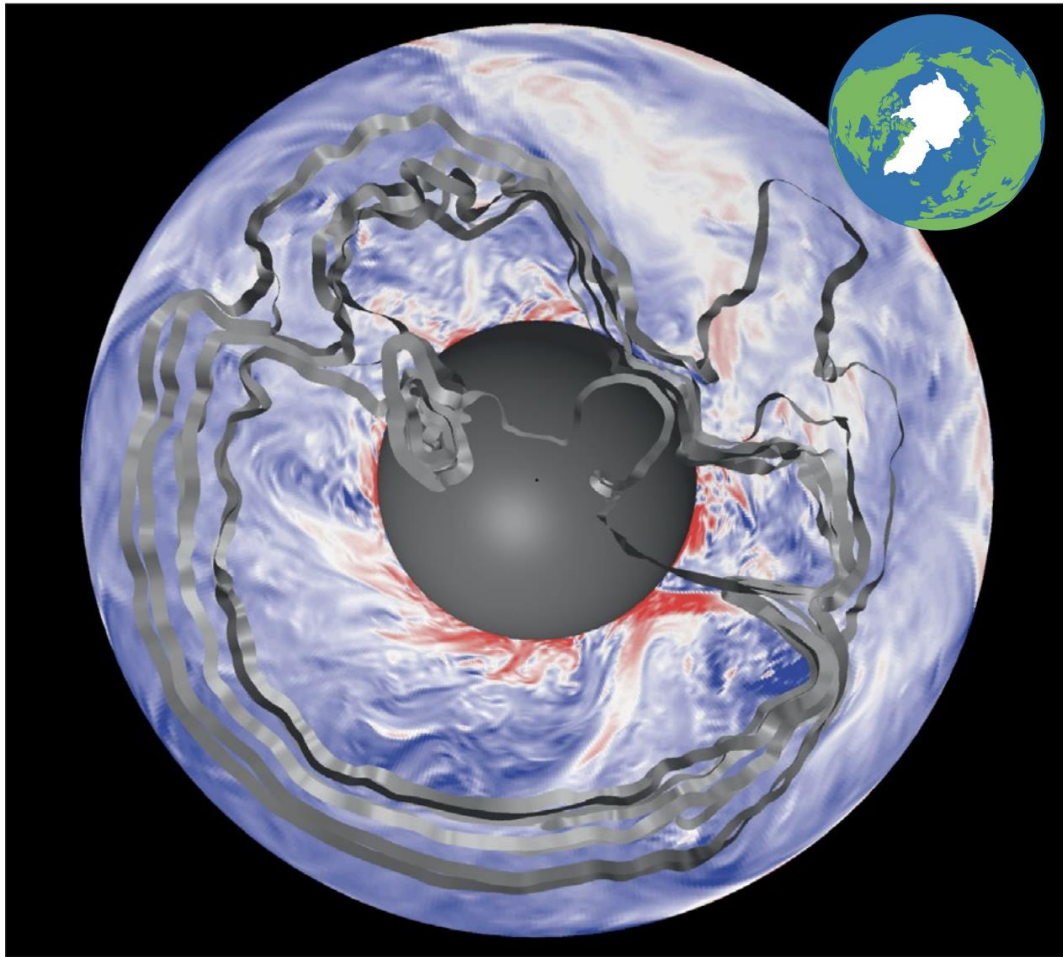
Pacific view



East-West Asymmetry of the Core Flow



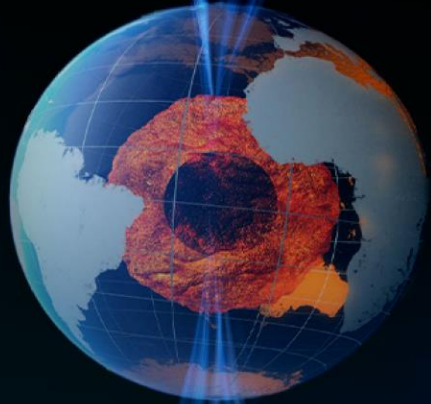
East-West Asymmetry of the Core Flow



Azimuthal velocity (km yr⁻¹)

40
20
0
-20
-40

- ❖ **We have developed a 3-D core flow inversion method based on the expansion of inertial modes and PINNs.**
- ❖ **The test experiments using the synthetic data show that it is possible to reconstruct large scale 3-D core flow.**
- ❖ **Preliminary 3-D core flow model derived from MSS-1 and Swarm data reveals the east-west hemispheric asymmetry in the core dynamics.**
- ❖ **The dynamical origin of the asymmetric core flow remains to be explored.**



SWARM

10

YEAR ANNIVERSARY
SCIENCE CONFERENCE

Thank you!



Swarm 10 Year Anniversary & Science Conference 2024